Testbeds for Integrated Transmission and Distribution Networks: Generation Methodology and Benchmarks

Jing Yu, *Student Member, IEEE*, Ye Guo, *Senior Member, IEEE*, and Hongbin Sun, *Fellow, IEEE*

***Abstract*—For future power systems with high penetration of distributed energy resources (DER), the coordination of the transmission system (TS) and distribution system (DS) is quite essential. In this paper, multiple testbeds that consist of various sizes of TS and DS models are designed for power flow (PF) and optimal power flow (OPF) analysis of the integrated transmission and distribution (T&D) systems. Several benchmarks with characteristics for applications are proposed and their simulation results are presented in this paper. Researchers can use the testbeds designed in this paper to build their specific cases with published data, and they can also compare the results of their new approaches or algorithms with those obtained by the proposed benchmarks in this paper.**

***Index Terms*—Distribution system, multi-area power systems, optimal power flow, power flow, test system design, transmission system.**

I. Introduction

A. Background

SINCE the penetration level of distributed energy resources (DER) is increasing at the distribution level, the outdated image that the transmission system (TS) hosts the supply side while the distribution system (DS) hosts the demand side is experiencing dramatic changes. With the increasing amount of distributed resources, the stakeholders at the distribution level are no longer pure consumers but have become capable of providing services for achieving better overall benefits. In other words, to enhance the security, competitiveness, and sustainability of the entire power system, the arrangements between the transmission system operator (TSO) and distribution system operator (DSO) require further revisions and developments to play a more active role in the following aspects [1], [2]: 1) exploring the flexibility on the distribution side to avoid the transformer congestion between the TS and DS; 2) managing the transmission line overload in the TS through integrating DER into the DS; 3) reducing the boundary imbalance caused by fluctuated distributed generations through TSO-DSO cooperation; 4) activating local flexibility to support the voltage of each other and enabling the coordinated protection.

There is a great deal of evidence in the policies and industry supporting the conclusion that in future power systems with high-level DER penetration, TSO-DSO coordination will become one of the key techniques [3]–[10]. For example, the agency for the cooperation of energy regulation (ACER) has published a report to call for improvement in the coordination between TSOs and DSOs [11]. Also, a report from the European Commission addressed a need for more coordination between the TSOs and DSOs, especially under the interconnection of smart grids in different EU member states [12]. At the same time, a large number of demonstration projects across the world have concentrated on enhancing DSO-TSO cooperation. For instance, the SMARTNET project has analyzed potential DSO-TSO coordination schemes [13]. Coincidentally, the Council of European Energy Regulators (CEER) also focused on the future DSO-TSO relationship, especially the related regulatory arrangements regarding planning and operation [14].

TSO-DSO coordination in recent years has also drawn extensive concern in academia. A series of research efforts have substantiated the necessity and benefits of TSO-DSO coordination [14]–[25]. The topics vary from the global power flow solution [16], [17], optimal power flow [18] and coordinated economic dispatch [19]–[21], to security analysis [22] hierarchical reactive power optimization [23] and static voltage stability assessment [24], etc. These investigations have widely facilitated the development of studies on TSO-DSO coordination.

However, one visible problem is that the comparisons between different achievements are still a non-trivial task due to the lack of widely accepted test systems for integrated transmission and distribution (T&D) systems. The reasons are manifold. First, the freely-designed integrated T&D systems for specific problems will be challenging for employment in other operational scenarios. In addition to that, the details on the connections between different systems have not received any special attention. Secondly, although there are already multiple separated transmission grids or distribution

Manuscript received December 4, 2019; revised April 21, 2020; accepted May 23, 2020. Date of online publication July 6, 2020; date of current version June 20, 2020.This work was supported in part by the National Key Research and Development Program of China under Grant 2018YFB0905000, in part by the National Natural Science Foundation of China (NSFC) under Grant 51537006 and 51977115.

J. Yu and Y. Guo are with the Shenzhen Environmental Science and New Energy Technology Engineering Laboratory Tsinghua-Berkeley Shenzhen Institute, Tsinghua University, Shenzhen, China.

H. B. Sun (corresponding author, e-mail: shb@tsinghua.edu.cn) is with the State Key Laboratory of Power Systems, Department of Electrical Engineering, Tsinghua University, Beijing 100084, China.

DOI: 10.17775/CSEEJPES.2019.03110

grid models with various structures [26]–[31], there are just a few specific test models designed for analyzing TSO-DSO interactions. One of them is the small-scale transmission and distribution (T&D) test system that consists of a six-bus TS and two active DSs in [32]. The other is an MATLAB toolbox named TDNetGen that was proposed to generate a series of open-source, parametrizable T&D test models [5], [33]. However, the common deficiency of the aforementioned T&D test models is that the choice of the separated model for TS and DS is simple and limited, which makes it difficult to represent the heterogeneity of different TSs and DSs. Therefore, for the reasons mentioned above, up to now, when researchers investigate the interplay between TS and DS or examine the specified algorithms designed for the co-operation or co-planning for TSO and DSO, there is a lack of reference T&D benchmarks that allow the testing and validation of the developed methods and algorithms for steady-state operations in the power system.

B. Contributions and Organization

In this paper, several integrated T&D benchmarks varying in scales and demand levels are designed for the steady-state analysis of TSO-DSO coordination. Specifically, the scope of application of these benchmarks primarily includes power flow calculation, contingency analysis, static voltage stability assessment, economic dispatch and other topics regarding steady-state power system operations.

The two primary purposes of this paper can be summarized as follows:

1) Provide a general method to construct highly-customizable T&D testbeds with separated TS and DS models, the underlying idea behind which is replacing the aggregated loads of TS by detailed DSs with similar demand levels. Researchers can freely generate various-size T&D test models for a variety of studies.

2) Provide four T&D benchmarks. The effectiveness of these systems was verified by figuring out reasonable power flow and optimal power flow solutions. The parameters and detailed results are provided in the template of MATPOWER for relevant studies, so that it is possible to compare and validate the performances of the newly proposed methods or algorithms relying on these publicly accessible data.

The remainder of this paper is organized as follows. In Section II, the basics of generating integrated T&D systems are introduced. Section III introduces the proposed T&D benchmarks. In Section IV, the results of the comparison between the distributed model and MATPOWER for some example testbeds are provided. Finally, some concluding remarks are presented in Section V.

II. Integrated T&D System Generation

In the real power grid, a TS is generally connected with several DSs [1], [2], so the newly generated integrated T&D systems are composed of one TS and several DSs. For more details, the separated TS and DS models, interconnecting substation, as well as the process of generating the combined T&D systems, are introduced in the remainder of this section.

A. TS Models

Five typical TS models used for generating the T&D benchmarks are listed in Table I from small to large scale. The basic information for these TS models, including the number of buses (Bus), branches (Bran.) and generators (Gen.), are summarized in Table I. Also, P and Q represent the total active and reactive power delivered to the demands.

TABLE I
SUMMARY OF TS MODELS

TS	Bus.	Bran.	Gen.	V (kV)	P (MW)	Q (MVAR)
T6 [32]	6	7	3	138	183.000	52.000
T30 [34]	30	41	6	135	189.200	107.200
T57 [34]	57	80	7	345-230-138	1295.400	362.900
T118 [34]	118	186	54	345-138	4242.000	1438.000
T300 [34]	300	411	70	345-66	23526.000	7788.000

For the smallest one, a meshed 6-bus TS model is designed based on that proposed in [32]. Then, all the other TS models are modified based on the widely-used IEEE test systems, which have already been published and provided in the data set of the latest version of MATPOWER.7.0b1 [34]. Notably, although IEEE 300 includes some nodes on the lower voltage level, only the nodes for transmission voltage levels can be selected as boundary buses.

B. DS Models

The models for DS varying in topology and load levels are given in Table II. First, the smallest two DS models, i.e., D7 and D9, are modified based on the DSs proposed in [32], which consist of 7 buses and 9 buses, respectively. The demand levels of these two systems are relatively high, representing the DSs that have seen a rapid growth of internal demand in recent years [35]. D33 is the widely-used radial 33-bus DS case [36]. Each DS model mentioned above consists of a single feeder. The fourth DS model DF3 is the three-feeder DS model provided in [37], and the tie-switches between the radial feeders are normally opened. Another looped 6-feeder DS model, called DF6, is modified based on the 44 kV DS provided by the Kingston public utility commission [38]. This model characterizes the area, wherein light industrial, commercial and civil load co-exist. Finally, a modified 77-bus DS system (DUK) based on the EHV1 generic model provided by the United Kingdom Generic Distribution System (UKGDS) is adopted. Full data for this rural meshed DS model is available in [28].

In addition to the scale information, the base voltage and load level of the DS models are summarized in Table II.

TABLE II
SUMMARY OF DS MODELS

DS	Bus.	Bran.	Feeder	Base voltage (kV)	Load level (MW)	Load level (MVar)
D7 [32]	7	4	1	69	62.000	16.390
D9 [32]	9	8	1	35	31.000	10.200
D33 [36]	33	37	1	12.66	3.715	2.300
DF3 [37]	16	13	3	23	28.700	8.900
DF6 [38]	44	38	6	44	59.300	17.800
DUK [28]	77	33	8	33	33.587	10.733

The detailed settings of the aforementioned cases are provided in [39], and all the DS cases enable us to obtain a

successful optimal power flow (OPF) solution by the primal-dual interior point solver (MIPS) of MATPOWER [34].

Additionally, since only the high-voltage or medium-voltage DSs that directly connect to the TS have been considered, it is reasonable to suppose that they are approximately three-phase balanced. Nonetheless, if researchers are willing to check the effectiveness of their methods or algorithms with larger scale or imbalanced DSs, the previous efforts [27], [40] can expand these options.

C. Interconnecting Substation

One of the main challenges of developing system models is that there are regional differences in the structure and operational circuits across the world, even though it is a fact that an electrical network normally is comprised of various voltage levels. In this paper, based on the aforementioned models of the TS and DSs, we hypothesize that a typical power system has the following voltage levels:

- Extra high voltage (EHV) transmission system: 345 kV and higher voltage level.
- Primary local transmission (or sub-transmission) system: from 66 kV to 230 kV systems.
- Distribution system: 35 kV and Lower.

Other realistic voltages are also possible, as long as the parameters are appropriately modified.

Then, in practice, the connection of a TS and the DSs is achieved by interconnecting substations (ICT), wherein transformers play a major role. The configurations of a transformer are determined by its primary (input) voltage and the secondary (output) voltage. To be specific, the medium-power transformers are typically defined as those connecting the primary side to the sub-transmission system and normally hold a capacity between 10 and 100 MVA [41], and in practice, they are used to move power between different parts of a county or city. According to the preceding assumption of the voltage levels, the medium-power transformers will be applied to connecting the TS and DSs mentioned in the previous subsections.

D. Generating T&D Testbeds

The basic idea of generating an integrated T&D testbed is replacing the original aggregated loads of a TS by detailed DSs. In this paper, the high-voltage and low-voltage busbars of an interconnecting substation are respectively defined as the boundary bus and feeder bus. Accordingly, the generating procedure started from the TS side is detailed as follows:

1) Selecting the boundary buses that are proposed to connect with DSs in the TS

After determine the total demand of a cluster that consists of several distribution feeders and DSs (The demand level of a DS is assigned to its base demand without considering any DER), the transmission bus with a similarly aggregated demand level as the boundary bus. In most cases, the scale of the integrated T&D system will be enlarged by more transmission buses being selected to connect with the DSs.

2) Defining the interconnecting substation

The main components in an ICT are one or two transformers, while the primary sides connect to the selected boundary bus, and the secondary side, are represented by the newly-defined feeder bus. The combination of these ensures the continuity between the TS and DSs, as shown in Fig. 1. Sometimes, the distribution feeders and DSs connected to the same boundary bus also share the same feeder bus, which represents the reality that multiple feeders start from an electrical substation.

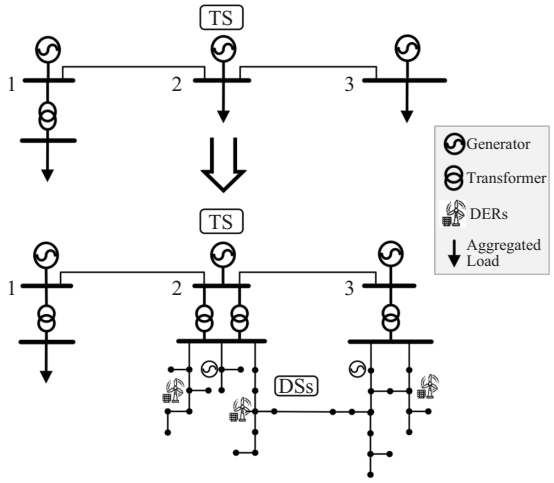

Fig. 1. Aggregated loads of the TS are replaced by detailed DSs.

3) Defining the feeder bus and modifying the DSs

Except for the bus type, the configurations of the feeder bus, are kept the same as those for the original slack bus in a distribution feeder or DS, while the feeder bus is specified as a PQ bus. From the perspective of the DS, after the connection, its previous slack bus is replaced by the connected feeder bus.

4) Constructing the joint T&D testbed

Completing the replacements on the selected transmission buses, a joint T&D testbed will be constructed. The newly-generated T&D cases can be expressed in MATPOWER format or converted into other standard mathematical optimization formats [31].

When this process is accomplished in MATLAB and exported in MATPOWER format, the cases can be directly used for PF and OPF simulations. The reasonable solutions obtained by MATPOWER can certainly prove the effectiveness of a newly-generated T&D testbed, and can be further applied in the analysis of TSO-DSO interaction and coordination. Moreover, if researchers are willing to check the effectiveness of their methods or algorithms on mass systems, they can also customize their T&D grids with separated models of the TS and DSs [26]–[30] following the proposed generation methods.

III. T&D Benchmarks

In this section, four integrated T&D benchmarks varying in scale and characteristics were constructed based on the idea of replacing the aggregated loads of a TS by detailed DSs. The demand level (i.e., the scope of the aggregated active load (P) and reactive load (Q) connected to transmission buses) of the five TSs are shown in Table III. It should be noted that in T300, only the positive aggregated demands connected to

nodes with voltage levels greater than or equal to 66 kV have been considered.

TABLE III
DEMAND SCOPES OF TS MODELS

TS	P (MW)	Q (MVAR)
T6	30–62	8–25
T14	3.5–94.2	1.6–19
T30	2.2–30	0.7–30
T118	2–277	1–113
T300	2.4–1019.2	0.4–598

The four benchmarks are T6-DF3, T30-DF6, T57-DUK, and T300-X, where the name before "–" represents the index of the specific TS presented in Table I, while after "–" is the index of DSs in Table II. Table IV shows the connection details.

TABLE IV
SUMMARY OF T&D TEST SYSTEMS

T&D Benchmarks	Bus ID with Boundary Bus	Number of Feeders/DSs
T6-DF3	(3, 4, 5)	(6, 6, 6)
T30-DF6	(5, 6, 8, 7, 9, 11)	(1, 1, 1, 1, 1, 1)
T57-DUK	(8)	(4)
T300-X	(9, 15, 23, 47, 48, 49, 55, 57, 63, 70, 77, 80, 218)	(3, 2, 7, 6, 6, 6, 5, 5, 5, 5, 5, 5, 4)

A more detailed introduction of each integrated T&D model is provided in the following sub-sections.

A. T6-DF3

The integrated system T6-DF3 consists of the 6-bus TS (i.e., T6), and the 3-feeder DS (i.e., DF3). The three feeders F1, F2, and F3 are connected with bus #4, #5, and #6 of the TS. Moreover, there are 6 copies of the feeders connected to each boundary bus. This T&D model is designed to represent the traditional power system, wherein several feeders connected to the same boundary bus of the distribution substation, and to simplify computing, none of the tie-switches are closed, which means the DSs, in this case, are considered operating in a radial topology. The topology of DF3 is shown below [37].

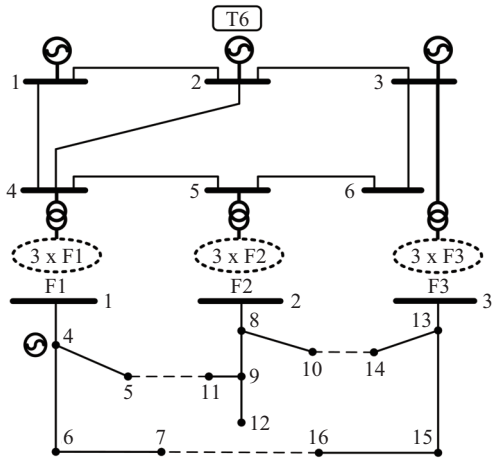

Fig. 2. Topology of DF3.

B. T30-DF6

This case is designed for the scenario, in which DSs are looped for reliability concerns. The topologies of the TS and DS that make up T30-DF6 are given by Fig. 3 and Fig. 4, respectively.

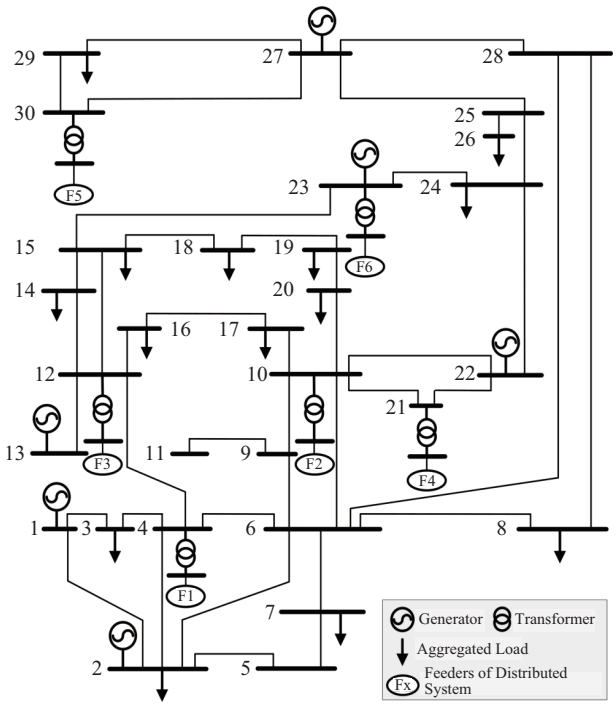

Fig. 3. Topology of T30.

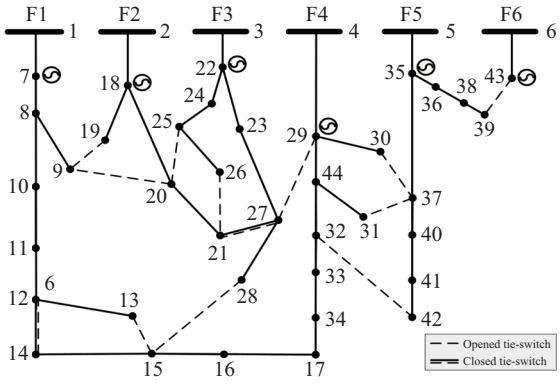

Fig. 4. Topology of DF6.

In T30-DF6, the six feeders of DF6 are separately connected to transmission bus # 4, #10, #12, #21, #30, and #23 of the T30. While unlike T6-DF3, two tie-switches in DF6 are closed to connect feeders from different boundary buses. To be more specific, feeder F1 and F4 of DF6 are interconnected, and so are feeder F2 and F3.

C. T57-DUK

In T57-DUK, T57 is selected as the TS and connected with four DUK at transmission bus #8, so there are five subsystems in this benchmark.

It is worth mentioning that this T&D case is designed for the scenario when a mass of DER are integrated into the DSs. For this purpose, in this case, we employed the real power penetration of RES as an index, which is defined as the ratio

of the active power injection from RES to the summation of active demand in a DS.

The topology of IEEE 57 is shown in Fig. 5.

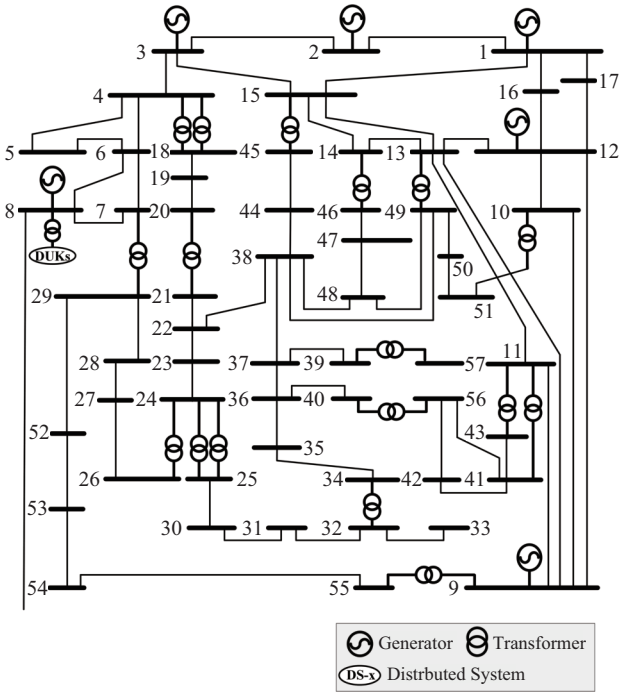

Fig. 5. Topology of T57.

The DUK is modified based on that proposed in [28], and for ensuring the reliability and stability of system operation, we combined some voltage levels to an integral value for simplification, i.e., in this case, the original TS voltage level of 132 kV has been categorized as 138 kV. Thus, the modified 33 kV distribution feeders are fed from a 138 kV supply point through two parallel-connected transformers. The diagram of DUK is shown in Fig. 6.

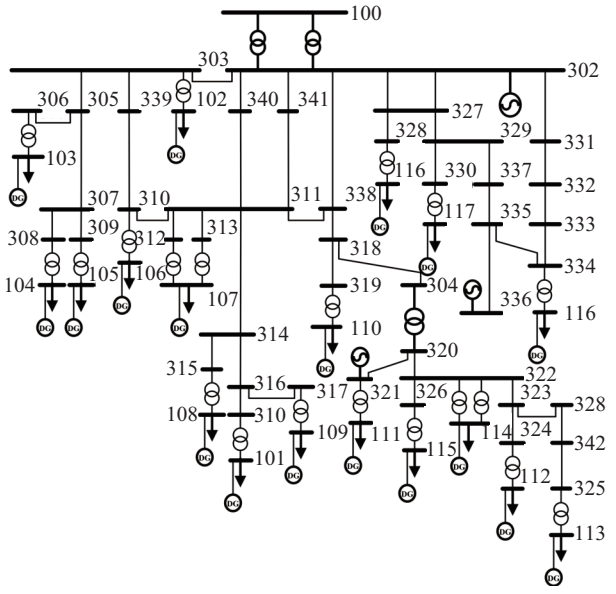

Fig. 6. Topology of DUK.

Additionally, DUK considered two types of DER, specifically, transmission bus #2, #21, and #36 are connected with a dispatchable DER, such as a hydraulic turbine, micro-turbine and fuel cell, which has excellent regulating performance to handle greater local demand. While the remaining load nodes were connected with non-controllable DER, especially renewable energy sources (RES) that usually include wind turbine generators (WTGs) and photovoltaic (PV) cells to serve residential demand. Although the output power of small capacity generation units is usually random and easily influenced by environmental factors, when they are clustered to form a wind farm or photovoltaic power plant, they can be used for grid dispatch as a whole and can even be treated as dispatchable DER.

D. T300-X

The T300-X is the largest test system designed in this paper, wherein 13 boundary buses of T300 are selected to connect with a total of 64 feeders or DSs. As a result, this integral T&D power system consists of 1089 buses, 1259 branches, and 152 controllable DER and 54 clusters of RES. The connection details are shown in Table V.

TABLE V
CONNECTION INFORMATION OF T300-X

Boundary Bus	Feeders / DSs	Number
9	D9	3
15	D7	2
23	D33	7
47	DF3-F1	6
48	DF3-F3	6
49	DF3-F2	6
55	DF6-F6	5
57	DF6-F5	5
63	DF6-F3	5
70	DF6-F1	5
77	DF6-F4	5
80	DF6-F2	5
218	DUK, DUK (30%), DUK (60%), DUK (90%)	1, 1, 1, 1

IV. SIMULATION RESULTS

It is worth noting that since the T&D test systems are constructed by connecting separated DSs to the TS, when connecting all the DSs to the TS, the original slack bus of a DS is no longer "slack" and has become the feeder bus. The transformers in the interconnecting substation are set to those with capacities ranging from 20 MVA to 100 MVA, and the impedances (per unit) referred to prime power ratings are mostly within 0.09 p.u. to 0.2 p.u. [42]. Also, in the benchmarks, transformers are set to work in the fixed-tap mode, and the tap ratios are indicated as per unit values. This value can be set to a value from 0.85–1.05 in the absence of other data. The power base in all cases is 100 MVA. All the details regarding the configurations of benchmarks are provided in [39]. Moreover, to improve the understandability after integration, the ID of other buses in the DSs have been redefined based on their connection relationship, and the method of renaming will be elaborated in subsequent subsections.

The IEEE 1547–2003 standard [43], defines DER as the units connecting to the DS with capacities of 10 MVA or

less. Meanwhile, according to the definition from the Electric Reliability Council of Texas (ERCOT) [44], DER are the electrical generating facilities (rating of 10 MW or less) located at the customer's points on a distribution feeder with a voltage level less than or equal to 60 kV. Thus, following these standards, in this paper, the capacities of the DER are less than 10 MW. Specifically, the capacities of the controllable DER in the distribution feeders followed the previous configurations in the original models.

All programs were coded and tested in MATLAB. We adopted the standard ACPF and ACOPF models for TSs and DSs, and the simulation results were executed by calling the "runpf.m" and "runopf.m" of MATPOWER 7.1.b. Moreover, MIPS has been selected as the solver of OPF problems [45]. For alternating current (AC) OPF, MIPS can usually provide a feasible power flow for the entire system and to some extent indicates that the settings of the test cases are reasonable for OPF calculation. To validate the effectiveness of the newly-built T&D benchmarks, the results of PF and OPF for these integrated systems are provided in separate charts.

A. T6-DF3

The integrated system T6-DF3 consists of the 6-bus TS and 18 radial feeders of DF3. For the ACPF calculation, we adopted the standard Newton-Raphson method in the polar coordinate [45]. The ACPF results, including voltage magnitudes and angles, are shown in Table VI. The explanation of the converted ID of distribution buses is that the first one (or first two in other cases) digit represents the bus ID of the connected transmission bus, and the following two digits are used to count the number of feeders connected to the same boundary bus, while the last two digits indicate the original bus ID in the previous DS.

TABLE VI
NODE VOLTAGE IN ACPF OF T6-DF3

Bus	Voltage (p.u.)	Angle (deg.)	Bus	Voltage (p.u.)	Angle (deg.)
1	1.000	0.000	8(40101)	1.024	−5.379
2	1.000	−3.398	40104	1.018	−5.515
3	1.000	−6.406	40105	1.014	−5.653
4	0.988	−3.985	40106	1.013	−5.810
5	0.987	−9.491	40107	1.012	−5.832
6	1.001	−7.206	9(50102)	1.043	−11.067
7(30103)	1.041	−7.488	50108	1.038	−11.414
30113	1.035	−7.575	50109	1.028	−11.903
30114	1.033	−7.620	50110	1.037	−11.443
30115	1.031	−7.703	50111	1.027	−11.933
30116	1.030	−7.729	50112	1.023	−12.125

From the perspective of the TS, the feeder buses seem like the additional transmission buses (i.e., bus #7 to #9), while they are also the replacements of the previous slack buses of the feeders. In addition to that, because of the existence of the transformers between the boundary buses, i.e., bus #4, #5 and #6, and the newly-built feeder buses, i.e., bus #7, #8 and #9, the magnitudes and angles of voltages on the two sides of the interconnecting substations were not exactly the same.

Table VII shows the results in terms of the active and reactive power flow on some branches after the ACPF calculation. The the branch start from bus #7, #8 and #9 indicate the newly-added virtual branches that represent the interconnecting substations connecting the TS and DSs.

TABLE VII
POWER FLOW IN ACPF OF T6-DF3

From	To	MW-flows	MVar-flows	From	To	MW-flows	MVar-flows
1	2	24.063	−13.152	4	8	27.245	17.495
1	4	34.042	−3.117	8	40104	4.541	2.762
2	3	20.284	−6.506	40104	40105	3.008	1.011
2	4	13.076	4.912	40104	40106	3.513	1.125
3	6	13.295	−4.447	40106	40107	1.501	0.501
4	5	19.190	−12.300	5	9	31.372	−3.529
5	6	−13.082	−2.769	9	50108	5.229	−0.734
3	7	21.777	13.357	50108	50109	10.199	2.636
7	30113	3.629	2.133	50108	50110	1.001	0.501
30113	30114	1.001	0.401	50109	50111	0.600	0.100
30113	30115	3.110	1.314	50109	50112	4.516	1.123
30115	30116	2.102	0.902				

In addition, the results of ACOPF are listed in Table VIII. In the case of a single objective function, i.e., minimizing operational cost, the voltage magnitudes and angles obtained by the ACOPF calculation were notably different with those from ACPF.

TABLE VIII
NODE VOLTAGE IN ACOPF OF T6-DF3

Bus	Voltage (p.u.)	Angle (deg.)	Bus	Voltage (p.u.)	Angle (deg.)
1	1.000	0.000	8	1.0551	−0.3931
2	1.002	−0.582	40104	1.0558	−0.3010
3	1.001	−1.857	40105	1.0524	−0.4299
4	1.005	−0.826	40106	1.0509	−0.5752
5	0.985	−5.261	40107	1.0501	−0.5960
6	1.001	−2.736	9	1.0355	−6.8512
7	1.053	−1.890	50108	1.0297	−7.1461
30113	1.052	−1.888	50109	1.0190	−7.6435
30114	1.051	−1.932	50110	1.0281	−7.1758
30115	1.049	−2.011	50111	1.0182	−7.6739
30116	1.048	−2.036	50112	1.0142	−7.8692

Table IX compares the results in terms of the active and reactive power outputs of generators in the different power flow calculations. For simplicity, "P" and "Q" are used as the abbreviations of "active power" and "reactive power" in the following table.

TABLE IX
POWER FLOW RESULTS OF T6-DF3

T6-DF3	Bus ID	P (MW)		Q (MVar)	
		PF	OPF	PF	OPF
TS	1	58.105	10.000	−16.269	−10.551
	2	10.000	7.393	8.965	−8.190
	3	15.000	6.767	10.476	−4.920
DF3-F1	40104, 40204, 40304 40404, 40504, 40604	4.000	10.000	0.000	2.318
DF3-F2	50108, 50208, 50308 50408, 50508, 50608	10.000	10.000	5.000	4.025
DF3-F3	30113, 30213, 30313 30413, 30513, 30613	1.500	5.000	0.000	1.976

From the above tables, all the results of PF and OPF obtained are reasonable, as there were no violations of operational constraints. While, unlike the OPF calculation, all generator limits, branch flow limits or voltage magnitude limits are ignored by the ACPF solvers of MATPOWER [45], so

that when the parameters are changed, some violations may occur, and more actions, such as bus type switching, should be applied to obtain a reasonable PF solution.

B. T30-DF6

The integrated system T30-DF6 is composed of the T30 and the 6-feeder meshed DS, i.e. the DF6. The ACPF results of T30-DF6 are shown in Table X.

TABLE X
POWER FLOW IN ACPF OF T30-DF6

Bus	Voltage (p.u.)	Bus	Voltage (p.u.)	Bus	Voltage (p.u.)
1	1.000	26	0.972	100221	1.006
2	1.000	27	1.000	120322	1.000
3	0.987	28	0.980	120323	1.002
4	0.984	29	0.987	120324	0.994
5	0.984	30	0.983	120325	0.990
6	0.978	31(40101)	1.013	120326	0.986
7	0.971	32(100202)	1.027	120327	1.003
8	0.966	33(120303)	1.007	120328	1.000
9	0.984	34(210404)	1.009	210429	1.000
10	0.988	35(300505)	1.012	210430	0.999
11	0.984	36(230606)	1.016	210431	0.989
12	0.985	40107	1.010	210432	0.985
13	1.000	40108	1.003	210433	0.976
14	0.976	40109	1.003	210434	0.973
15	0.980	40110	0.992	300535	1.010
16	0.978	40111	0.980	300536	1.007
17	0.980	40112	0.973	300537	1.004
18	0.970	40113	0.970	300538	1.002
19	0.967	210414	0.971	300539	1.001
20	0.971	210415	0.970	300540	0.993
21	0.994	210416	0.970	300541	0.985
22	1.000	210417	0.971	300542	0.983
23	1.000	100218	1.030	230643	1.010
24	0.988	100219	1.028	210444	0.990
25	0.990	100220	1.010		

For clarity, in this case, the two digits in the middle of the bus ID represent the feeder ID, e.g., the nomenclature here is that in "40101", "4" is the transmission bus ID, "01" means the F1 of the DF6, and for the last two digits "01" is the previous bus ID in the DS. As shown in Table X, all the obtained voltage magnitudes were within the operation interval consists of the lower and upper bounds.

Table XI compares the active power flow at some branches obtained by ACPF and DCPF. Although there were some differences, the changing trends in both cases were similar. The last night branches are tie-lines and closed tie-switches. Moreover, in this case, the operational cost of the reactive power has also been taken into account.

In addition, from the OPF results shown in Table XII, it is easy to conclude that after the OPF calculations, to meet the same active demand, the real power outputs of the generators in both cases were roughly the same. In the meantime, in the ACOPF calculation, not only the power losses but also the generation cost regarding the reactive power has been taken into account [45].

C. T57-DUK

T57-DUK is specially designed for the scenarios with high RES penetration. To be specific, each demand point has been connected with a cluster of RES. For the sake of uniformity for comparison, the simulations were performed at different

TABLE XI
POWER FLOW RESULTS OF T30-DF6

Branch	MW-Flows		Branch	MW-Flows	
i–j	ACPF	DCPF	i–j	ACPF	DCPF
1–2	−14.528	−16.821	10–17	4.417	4.513
1–3	0.945	0.251	10–21	−11.019	−11.064
2–4	6.425	5.712	10–22	−7.145	−7.308
3–4	−1.478	−2.149	21–22	−15.470	−16.088
2–5	8.889	8.339	15–23	−11.063	−11.076
2–6	9.381	8.397	22–24	−1.150	−1.807
4–6	14.578	13.511	23–24	6.899	7.124
5–7	8.833	8.339	24–25	−3.078	−3.382
6–7	14.099	14.461	25–26	3.546	3.500
6–8	23.347	23.294	25–27	−6.646	−6.882
6–9	−4.464	−5.743	28–27	−13.438	−13.528
6–10	−2.551	−3.282	27–29	3.508	3.388
9–11	0.000	0.000	27–30	3.268	3.112
9–10	−4.464	−5.743	29–30	1.077	0.988
4–12	−14.023	−13.023	8–28	−6.773	−6.706
12–13	−37.000	−37.000	6–28	−6.611	−6.822
12–14	4.871	4.780	4–40101	4.334	3.075
12–15	7.364	7.376	10–100202	0.477	−1.235
12–16	8.196	7.987	12–120303	2.545	3.835
14–15	−1.360	−1.420	21–210404	4.408	5.025
16–17	4.634	4.487	30–300505	4.303	4.100
15–18	8.823	8.832	23–230606	1.093	1.000
18–19	5.534	5.632	40112–210414	4.334	3.075
19–20	−3.986	−3.868	100221–120327	0.477	−1.235
10–20	6.255	6.068			

TABLE XII
OPTIMAL POWER FLOW RESULTS OF T30-DF6

T30-DF6	Bus ID	P (MW)		Q (MVar)	
		ACOPF	DCOPF	ACOPF	DCOPF
TS	1	17.952	23.489	20.326	–
	2	35.383	30.389	14.389	–
	13	0.000	0.000	12.080	–
	22	46.889	28.721	10.715	–
	23	23.644	30.000	9.582	–
	27	31.695	40.000	9.892	–
DF6-F1	40107	0.000	0.000	1.200	–
DF6-F2	100218	5.000	5.000	1.500	–
DF6-F3	120322	10.000	10.000	3.500	–
DF6-F4	210429	10.000	10.000	3.500	–
DF6-F5	300535	10.000	10.000	4.000	–
DF6-F6	230643	5.000	5.000	1.500	–
Cost ($)		2860.774	2783.498	560.632	–

RES penetrations in different DUKs that were connected to the same transmission bus, while guaranteeing there was no overvoltage or overcurrent at any node of the integrated T&D system. There were four DUKs with RES penetration from 0% (the base case) to 90% in steps of 30%, which were connected together to the transmission bus #8. The variations in the RES penetration also represented the intermittent and unpredictable properties of RES generations.

Furthermore, there are various choices of RES, while in this case, we put more focus on WTGs. The reasons are that the technologies of WTG have advanced significantly over the past few years with a developed capacity from the order of kilowatts to several megawatts. Currently, for higher stability and efficiency, several WTGs can compose a wind power plant (WPP) that was built in a high-voltage DS, such as the DS with a system voltage of 34.5 kV in North America [46], which is much more suitable for the integrated T&D considered in this paper. Additionally, according to a report from the IEEE PES Wind Plant Collector System Design Working Group [47], the modern WPPs are required to have the capacity of generating

reactive power over a specified range of power factor, for instance, from 0.9 leading (inductive) to 0.9 lagging (capacitive), which means the nodes connected with WPPs can be regarded as PQ buses. Accordingly, in this case, WPPs were regarded as negative loads with a specific power factor of 0.95.

The ACPF results of T57-DUK, in terms of the voltage magnitudes, are shown in Fig. 7, which intuitively illustrates that the obtained voltage magnitudes of all buses were within the operational ranges. In addition to that, when keeping the same generation of the controllable generators, higher RES penetrations obviously increased the local voltage magnitude in the DS, due to the reactive capacity provided by WPPs.

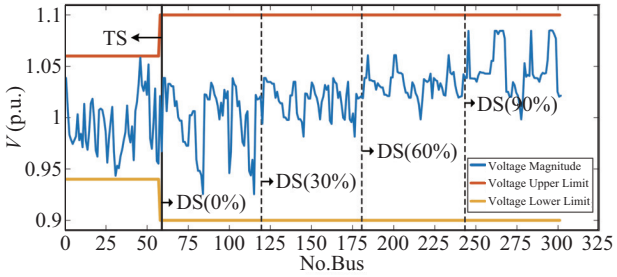

Fig. 7. Voltage magnitudes in ACPF of T57-DUK.

The ACOPF results, regarding the voltage magnitudes and active generations for TS, are shown in Fig. 8.

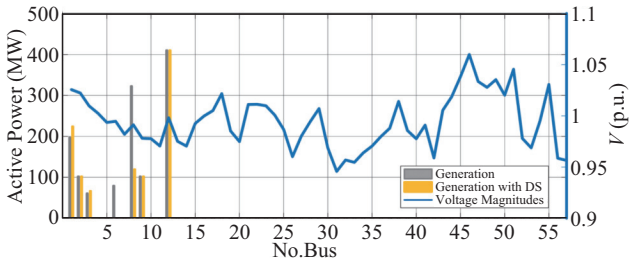

Fig. 8. Voltage magnitudes and active generations in ACOPF of T57.

The figure above is only meant to show the impacts placed by the DSs with high RES penetrations on the TS. Indeed, as shown in Fig. 8, the integration of the RES has directly influenced the operation of the TS, which is intuitively reflected in the active outputs of the large-scale generators in the TS. Therefore, especially in high-level RES penetrations scenarios, the coordination between separated systems and accurate predictions will play more critical roles.

The types of RES can be freely modified, as long as their capacities are roughly less than 10 MW. Also, the reactive capability of RES varies according to the categories of the devices. Specifically, according to the mechanism and operational characteristics of RES, the node connected with the RES devices may also be modeled as a P(Q) V or PI bus in the power flow calculation.

D. T300-X

The T300-X is the largest benchmark, which consists of the IEEE 300 TS and 64 distribution feeders and DSs, so there are 65 subsystems in this integral T&D system. Moreover, all the tie-switches are opened and the DSs are in radial topologies.

The ACPF results for the voltage magnitudes of 1089 buses are shown in Fig. 9, in which the curve in blue represents the obtained voltage magnitudes of all buses that were within the specified operation interval.

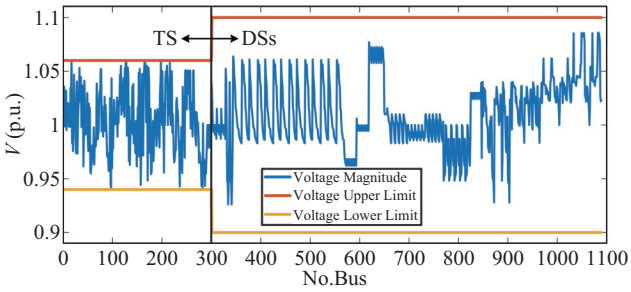

Fig. 9. Voltage magnitudes in ACPF of T300-X.

Additionally, Table XIII shows the ACOPF results for this large-scale benchmark, in terms of the voltage magnitudes of the boundary buses and feeder buses on the two sides of the interconnecting substations. Meanwhile, the active and reactive power injections into the feeder buses from the transmission buses are also provided.

TABLE XIII
ACOPF RESULTS OF CASE T300-X

Transmission Bus	Voltage (p.u.)	Feeder Bus	Voltage (p.u.)	Active Power (MW)	Reactive Power (MW)
9	1.041	301	1.072	18.819	1.742
15	1.048	302	1.081	72.323	1.093
23	1.030	303	1.060	−42.755	37.894
47	1.033	304	1.045	−8.874	0.459
48	1.043	306	1.075	31.347	−11.999
49	1.060	306	1.075	31.347	−11.999
55	1.060	307	1.075	0.000	0.040
57	1.008	308	1.090	21.367	2.975
63	1.036	309	1.093	5.401	−0.501
70	1.021	310	1.004	13.142	5.960
77	1.060	311	1.059	29.916	9.679
80	1.054	312	1.063	5.576	1.651
218	1.034	313	1.015	9.986	−5.109
		314	1.015	−2.126	−6.568
		315	1.015	−13.821	0.156
		316	1.015	−25.163	−8.832

It was determined that when the connected DSs integrated more DER's generations than their local demands, they would create reverse power flows from the corresponding feeder buses to the connected boundary buses in the TS, which may place significant challenges on the TS-side operation. Thus, in the face of such changeable boundary states, to explore the potential for a better dispatch of the entire power system, the coordination of the operators of the separated systems becomes particularly necessary.

V. CONCLUSION

In this paper, some benchmarks for the integrated T&D system have been proposed. The data of the cases are provided to the public for the following researches on the coordination of the TS and DSs. Based on the simulations by MATLAB and

MATPOWER, the effectiveness of the newly-built benchmarks has been certainly validated. Meanwhile, the obtained ACOPF results by MIPS actually provided an upper bound for the ACOPF solution.

More improvements can be made based on the current versions of the models. For example, the proposed benchmarks can be further developed to incorporate more practical network devices, such as energy storage, voltage regulator, etc.. Also, more demand-based approaches, such as demand response and demand-side management can be taken into account. Besides, the scenarios considering imbalanced distribution feeders and more precisely large-scale integrated T&D systems are also worth further investigations.

REFERENCES

[1] H. B. Sun, "The studies on global reactive optimal control of power system," Ph. D. dissertation. Tsinghua University, Beijing, China, 1996.

[2] Z. S. Li, Distributed Transmission-Distribution Coordinated Energy Management Based on Generalized Master-Slave Splitting Theory, Singapore: Springer, 2018, pp. 1–15.

[3] M. Birk, J. P. Chaves-Ávila, T. Gómez, and R. Tabors. "TSO/DSO coordination in a context of distributed energy resource penetration," in *TSO/DSO Coordination in a Context of Distributed Energy Resource Penetration*, 2017.

[4] MT, "Coordination of transmission and distribution operations in a high distributed energy resource electric grid," MTS, Aug. 2017.

[5] P. Aristidou, G. Valverde, and T. Van Cutsem, "Contribution of distribution network control to voltage stability: a case study," *IEEE Transactions on Smart Grid*, vol. 8, no. 1, pp. 106–116, Jan. 2017.

[6] M. Heleno, R. Soares, J. Sumaili, R. J. Bessa, L. Seca, and M. A. Matos, "Estimation of the flexibility range in the transmission-distribution boundary," in *IEEE Eindhoven PowerTech*, Jun. 2015, pp. 1–6.

[7] ENTSO (European Network of Transmission System Operators). (2015, Nov 9). General guidelines for reinforcing the cooperation between TSOs and DSOs. [Online]. Available: https://www.entsoe.eu/2015/11/09/general_guidelines_for_reinforcing_the_cooperation_between_tsos_and_dsos/.

[8] J. Villar, R. Bessa, and M. Matos, "Flexibility products and markets: literature review," *Electric Power Systems Research*, vol. 154, pp. 329–340, Jan. 2018.

[9] I. J. Perez-Arriaga, "The transmission of the future: the impact of distributed energy resources on the network," *IEEE Power and Energy Magazine*, vol. 14, no. 4, pp. 41–53, Jul.-Aug. 2016.

[10] A. Zegers and H. Brunner, "TSO-DSO interaction: an overview of current interaction between transmission and distribution system operators and an assessment of their cooperation in smart grids," International Smart Grid Action Network, International Smart Grid Action Network Discussion Paper, Sep. 2014.

[11] ACER (Agency for the Cooperation of Energy Regulation). (2013, Nov 7). "A bridge to 2025" publication proposals for future roles of DSOs. [Online]. Available: https://acer. europa. eu.

[12] European Commission. (2018, Feb. 26). Workshop on digitizing the energy value chain. [Online] Available: https://ec.europa.eu.

[13] H. Gerard, E. I. R. Puente, and D. Six, "Coordination between transmission and distribution system operators in the electricity sector: a conceptual framework," *Utilities Policy*, vol. 50, pp. 40–48, Feb. 2018.

[14] CEER (Council of European Energy Regulators). (2016, Sep. 21). CEER position paper on the future DSO and TSO relationship. [Online]. Available: https://www.ceer.eu.

[15] Z. S. Li, H. B. Sun, Q. L. Guo, J. H. Wang, and G. Y. Liu, "Generalized master–slave-splitting method and application to transmission–distribution coordinated energy management," *IEEE Transactions on Power Systems*, vol. 34, no. 6, pp. 5169–5183, Nov. 2019.

[16] H. B. Sun, Q. L. Guo, B. M. Zhang, Y. Guo, Z. S. Li, and J. H. Wang, "Master-slave splitting based distributed global power flow method for integrated transmission and distribution analysis," *IEEE Transactions on Smart Grid*, vol. 6, no. 3, pp. 1484–1492, May 2015.

[17] Q. H. Huang and V. Vittal, "Integrated transmission and distribution system power flow and dynamic simulation using mixed three-sequence/three-phase modeling," *IEEE Transactions on Power Systems*, vol. 32, no. 5, pp. 3704–3714, Sep. 2017.

[18] Z. S. Li, Q. L. Guo, H. B. Sun, and J. H. Wang, "Coordinated transmission and distribution AC optimal power flow," *IEEE Transactions on Smart Grid*, vol. 9, no. 2, pp. 1228–1240, Mar. 2018.

[19] Z. S. Li, Q. L. Guo, H. B. Sun, and J. H. Wang, "Coordinated economic dispatch of coupled transmission and distribution systems using heterogeneous decomposition," *IEEE Transactions on Power Systems*, vol. 31, no. 6, pp. 4817–4830, Nov. 2016.

[20] J. Yu, Z. S. Li, Y. Guo, and H. B. Sun, "Decentralized chance-constrained economic dispatch for integrated transmission-district energy systems," *IEEE Transactions on Smart Grid*, vol. 10, no. 6, pp. 6724–6734, Nov. 2019.

[21] Y. Guo, L. Tong, W. C. Wu, B. M. Zhang, and H. B. Sun, "Coordinated multi-area economic dispatch via critical region projection," *IEEE Transactions on Power Systems*, vol. 32, no. 5, pp. 3736–3746, Sept. 2017.

[22] Z. S. Li, J. H. Wang, H. B. Sun, and Q. L. Guo, "Transmission contingency analysis based on integrated transmission and distribution power flow in smart grid," *IEEE Transactions on Power Systems*, vol. 30, no. 6, pp. 3356–3367, Nov. 2015.

[23] R. Venkatraman, S. K. Khaitan, and V. Ajjarapu, "Dynamic co-simulation methods for combined transmission-distribution system with integration time step impact on convergence," *IEEE Transactions on Power Systems*, vol. 34, no. 2, pp. 1171–1181, Mar. 2019.

[24] Z. S. Li, Q. L. Guo, H. B. Sun, J. H. Wang, Y. L. Xu, and M. Fan, "A distributed transmission-distribution-coupled static voltage stability assessment method considering distributed generation," *IEEE Transactions on Power Systems*, vol. 33, no. 3, pp. 2621–2632, May 2018.

[25] Q. H. Huang and V. Vittal, "Advanced EMT and phasor-domain hybrid simulation with simulation mode switching capability for transmission and distribution systems," *IEEE Transactions on Power Systems*, vol. 33, no. 6, pp. 6298–6308, Nov. 2018.

[26] A. B. Birchfield, K. M. Gegner, T. Xu, K. S. Shetye, and T. J. Overbye, "Statistical considerations in the creation of realistic synthetic power grids for geomagnetic disturbance studies," *IEEE Transactions on Power Systems*, vol. 32, no. 2, pp. 1502–1510, Mar. 2017.

[27] K. P. Schneider, B. A. Mather, B. C. Pal, C. W. Ten, G. J. Shirek, H. Zhu, J. C. Fuller, J. L. R. Pereira, L. F. Ochoa, L. R. de Araujo, R. C. Dugan, S. Paudyal, T. E. McDermott, and W. Kersting, "Analytic considerations and design basis for the IEEE distribution test feeders," *IEEE Transactions on Power Systems*, vol. 33, no. 3, pp. 3181–3188, May 2018.

[28] Distributed Generation and Sustainable Electrical Energy Centre: United Kingdom Generic Distribution System (UK GDS). [Online]. Available: http://www.sedg.ac.uk/.

[29] K. Strunz, E. Abbasi, R. Fletcher, and N. D. Hatziargyriou, "Benchmark systems for network integration of renewable and distributed energy resources," CIGRE, Cigre TF C6.04.02/TB 575, Apr. 2014.

[30] A. M. Stanisavljević, V. A. Katić, B. P. Dumnić, and B. P. Popadić, "A brief overview of the distribution test grids with a distributed generation inclusion case study," *Serbian Journal of Electrical Engineering*, vol. 15. No. 1, pp. 115–129, Feb. 2018.

[31] C. Josz, S. Fliscounakis, J. Maeght, and P. Panciatici, "AC power flow data in MATPOWER and QCQP format: iTesla, RTE snapshots, and PEGASE," arXiv preprint arXiv: 1603.01533, pp. 1–7, Mar. 2016.

[32] A. Kargarian and Y. Fu, "System of systems based security-constrained unit commitment incorporating active distribution grids," *IEEE Transactions on Power Systems*, vol. 29, no. 5, pp. 2489–2498, Sep. 2014.

[33] N. Pilatte, P. Aristidou, and G. Hug, "TDNetGen: an open-source, parametrizable, large-scale, transmission, and distribution test system," *IEEE Systems Journal*, vol. 13, no. 1, pp. 729–737, Mar. 2019.

[34] R. D. Zimmerman and C. Murillo-Sánchez. MATPOWER User's Manual. [Online]. Available: http://www.pserc.cornell.edu/matpower/.

[35] A. Azizivahed, M. Barani, S. E. Razavi, S. Ghavidel, L. Li, and J. F. Zhang, "Energy storage management strategy in distribution networks utilised by photovoltaic resources," *IET Generation, Transmission & Distribution*, vol. 12, no. 21, pp. 5627–5638, Nov. 2018.

[36] M. E. Baran and F. F. Wu, "Network reconfiguration in distribution systems for loss reduction and load balancing," *IEEE Transactions on Power Delivery*, vol. 4, no. 2, pp. 1401–1407, Apr. 1989.

[37] S. Civanlar, J. J. Grainger, H. Yin, S. S. H. Lee, "Distribution feeder reconfiguration for loss reduction," *IEEE Transactions on Power Delivery*, vol. 3, no. 3, pp. 1217–1223, Jul. 1988.

[38] T. P. Wagner, A. Y. Chikhani, R. Hackam, "Feeder reconfiguration for loss reduction: an application of distribution automation," *IEEE Transactions on Power Delivery*, vol. 6, no. 4, pp. 1922–1933, Oct. 1991.

[39] Data for the benchmarks. [Online]. Available: https://drive. google. com/drive/folders/1Ast4MIcarOo8EJFu94L4OJ7ocJlZTaBH?usp=sharing.
[40] SMART-DS: synthetic models for advanced, realistic testing: distribution systems and scenarios. [Online]. Available: https://www.nrel. gov/grid/smart-ds. html.
[41] P. Upadhyay, S. Englebretson, and V. R. R. Ramanan. Novel concept for flexible and resilient large power transformers. ABB Inc. Final Technical Report. [Online]. Available: https://www.osti.gov/servlets/purl/1435970.
[42] Horizon Power. 2015. Specification-substation power transformer. [Online]. Available: https://horizonpower. com. au/media/1613/hpc-8dc-23-0001-2015-spec-substation-power-transformer. pdf.
[43] *IEEE standard for interconnecting distributed resources with electric power systems*, IEEE Standard 1547–2003, 2003.
[44] Distributed Generation. ERCOT, (2017). [Online]. Available: http://www.ercot.com/services/rq/re/dgresource.
[45] R. D. Zimmerman, C. E. Murillo-Sánchez, and R. J. Thomas, "MATPOWER: steady-state operations, planning, and analysis tools for power systems research and education," *IEEE Transactions on Power Systems*, vol. 26, no. 1, pp. 12–19, Feb. 2011.
[46] E. H. Camm, M. R. Behnke, O. Bolado, M. Bollen, M. Bradt, C. Brooks, W. Dilling, M. Edds, W. J. Hejdak, D. Houseman, S. Klein, F. Li, J. Li, P. Maibach, T. Nicolai, J. Patino, S. V. Pasupulati, N. Samaan, S. Saylors, T. Siebert, T. Smith, M. Starke, and R. Walling, "Wind power plant collector system design considerations: IEEE PES wind plant collector system design working group," in *Proceedings of 2009 IEEE Power & Energy Society General Meeting*, Calgary, AB, 2009, pp. 1–7.
[47] E. H. Camm, M. R. Behnke, O. Bolado, M. Bollen, M. Bradt, C. Brooks, W. Dilling, M. Edds, W. J. Hejdak, D. Houseman, S. Klein, F. Li, J. Li, P. Maibach, T. Nicolai, J. Patino, S. V. Pasupulati, N. Samaan, S. Saylors, T. Siebert, T. Smith, M. Starke, and R. Walling, "Characteristics of wind turbine generators for wind power plants," in: *Proceedings of 2009 IEEE Power & Energy Society General Meeting*, Calgary, AB, 2009, pp. 1–5.

Jing Yu (S'18) received the first B.S. degree from the University of Manchester, U.K., and the second B.S. degree from North China Electric Power University, Beijing, China, in 2016. She is currently pursuing the Ph.D. degree with Tsinghua-Berkeley Shenzhen Institute, Shenzhen, China. Her current research interests include the coordination of smart transmission and distribution grids, and distributed storage utilization in integrated energy system.

Ye Guo (SM'18) received the B.E. and Ph.D. degrees in 2008 and 2013, respectively, from the Electrical Engineering Department, Tsinghua University. He was a postdoctoral research associate at Cornell University from 2014 to 2018. Currently, he is an Assistant Professor at Tsinghua-Berkeley Shenzhen Institute. His research interests include power system economics, power system state estimation, decentralized optimization for multi-area power systems, and the integration of renewable generations and storages.

Hongbin Sun (SM'12–F'18) received the double B.S. degrees from Tsinghua University in 1992, and his Ph.D. from the Department of Electrical Engineering, Tsinghua University in 1997. He is now a Changjiang Scholar of the Education Ministry of China, Full Professor of Electrical Engineering at Tsinghua University and Assistant Director of the State Key Laboratory of Power Systems in China. From September 2007 to September 2008, he was a visiting professor with the School of EECS at Washington State University in Pullman, Washington, USA. During the past 20 years, he led a research group at Tsinghua University in developing a commercial system-wide automatic voltage control system, which has been applied to the PJM interconnection, the largest regional power grid in the USA, and to more than 60 large-scale power grids in China. He published more than 300 academic papers. His research interests include smart grids, renewable generation integration, and electrical power control center applications.